Environ Geol (2006) 50: 725–742
DOI 10.1007/s00254-006-0245-x

ORIGINAL ARTICLE

L. Horckmans
R. Swennen
J. Deckers

Geochemical and mineralogical study of a site severely polluted with heavy metals (Maatheide, Lommel, Belgium)

Received: 13 October 2005
Accepted: 26 February 2006
Published online: 28 March 2006

L. Horckmans (✉) · R. Swennen
Geologie, K.U. Leuven,
Celestijnenlaan 200E,
3001 Heverlee, Belgium
E-mail:
Liesbeth.Horckmans@geo.kuleuven.be
Tel.: +32-16-327807
Fax: +32-16-327981

J. Deckers
Afdeling Bodem- en Waterbeheer,
K.U. Leuven, Celestijnenlaan 200E,
3001 Heverlee, Belgium

Abstract The former zinc smelter site 'de Maatheide' in Lommel (Belgium) was severely polluted with heavy metals and the pollution spread into the surroundings by rain water leaching and wind transportation. This study focuses on the processes of immobilization and natural attenuation that took place on the site. Three important factors were found. Firstly, the high pH values (pH 7–8) in the topsoil influence the mobility of heavy metals. Secondly, the spodic horizons below the polluted top layer seem to accumulate heavy metals, thereby slowing down their release into the environment. Finally, the glassy phases and iron oxi/hydroxides that are present can encapsulate heavy metals during their formation/recrystallization, thereby immobilizing them. An additional shielding effect results from the reaction rims of goethite around the contaminant phases, which partially inhibit the weathering process and release of contaminants. This shielding effect is an important factor to take into account when modelling contaminant release.

Keywords Heavy metals · Sandy soils · Natural attenuation · Zinc smelter · Mineralogy · Belgium · Campine · Lommel

Introduction

Large areas in the northern Campine (Belgium) suffer from soil pollution with heavy metals, due to the non-ferro metal industry that was founded in that area in the nineteenth century. The sandy, infertile soils that are the dominant soil type in this region, are in general unsuitable for agriculture and hence ground prices were, and are still, very low. Population density was also very low, making the area ideally suited for the highly polluting non-ferro metal industry. Low labour cost and good infrastructure provided additional benefits (Anonymous 1990). Many of these zinc and other metal smelters have been closed in the past decades, while in the remaining factories production processes have been modernized so that the emission of heavy metals has been drastically reduced. However, the sites of former and present day zinc smelters in this region are known point sources for the spread of heavy metals in the environment by wind transportation of polluted particles and/or rain water leaching (Vangronsveld et al. 1995a). An inventory of the distribution of heavy metals in the soils of the Campine by Bosmans and Paenhuys (1980) clearly showed increased concentrations of heavy metals in the vicinity of the non-ferro metal industry. Of importance here is that the low buffering capacity of the sandy soils causes metals to be easily leached into the groundwater. The annual rainfall in the northern Campine lies around 800 mm, the topography is mostly flat and winds are dominantly south-west oriented.

Due to the large number of polluted soils in the northern Campine, remediation of all affected sites is not an option, especially since most of them are very diffusely polluted. Therefore, attention is also given to alternative methods of heavy metal retention, and the effect of natural attenuation processes. Such alternatives

are especially promising towards diffusely polluted sites, instead of severely polluted sites where remediation often is imminent. However, this study focuses on a highly polluted site where attenuation processes can be identified more easily.

The study area is 'de Maatheide' in Lommel, where 70 years of zinc smelting (1904–1974) left a heavily polluted soil with high concentrations of Zn, Pb, Cu and Cd. Recently, the site has been remediated, but at the time of this study, polluted soils covered a surface area of 135 ha (Fig. 1). In the top soil Zn concentrations locally exceeded 10 g/kg (Vangronsveld et al. 1995b). The dominant source of heavy metals is the slag material, which was spread out over the industrial site after the zinc smelter ceased industrial activity and was demolished in 1974. In the early 1950s, municipal waste was dumped on the site in order to improve the soil structure (Anonymous 1990), but no further environmental management practices were carried out at the time. As a consequence, several unstable mineral phases weathered and a number of secondary phases formed. The pollution spread into the subsurface and the groundwater became polluted (Steenackers 1991). Vegetation was in general very scarce and consisted mostly of metal tolerant Lichenes and Bryophyta; 10% of the area was completely bare. In 1990, a study by Vangronsveld et al. (1995a, b) aimed at the restoration of a vegetative cover by adding a metal immobilizing substance, beringite, to the soil after removal of stones and concrete material with a diameter >2 cm, and sowing metal-tolerant plants on the experimental plot (3 ha). It was shown that the addition of beringite significantly lowered the symptoms of metal phytotoxicity in the plants, and that a vegetative cover could be restored. An evaluation 5 years later showed that phytotoxicity was maintained at a low level, and that the water-extractable metal fraction of the treated soil was up to 70 times lower compared to the untreated soil (Vangronsveld et al. 1996). Later studies showed that this effect is probably mainly due to an increase in pH (Lombi et al. 2002a, b, 2003). Recently, a study with single extractions and XAFS also showed that the speciation of Zn and Cd did not differ significantly between the remediated and unremediated soils (D. L. Sparks 2005, personal communication).

In general, however, the site was left largely unattended for about 30 years, which allows the study of natural processes on this time scale. Another factor that made the site interesting for the study of natural attenuation, is the presence of original, partly preserved, soil profiles (mainly Podzols) below a highly polluted top layer, making it possible to study both the behaviour of the mineral phases at the surface, where neo-formation of mineral phases and leaching of heavy metals occurs, and the fate of these leached metals in the underlying soils over a time interval of about 30 years. Finally, at certain locations on the site, especially along the former roads, an indurated 'iron crust' with a thickness varying

Fig. 1 Photograph of the site before remediation

from a few cm to 35 cm is present above the sandy soils. They relate to crushed and subsequently weathered ash material, and are the result of dissolution/precipitation reactions involving rain water and subsequent consolidation/lithification of the different fragments. Their role in immobilizing heavy metals was also investigated.

The first aim of this study was to make an inventory of the areal extent of the pollution. The second aim is to report on the geochemical as well as the petrographical/mineralogical characterization of the heavily polluted top soil, including the iron crusts, with special attention to the formation of secondary phases. Thirdly, some profiles beneath the polluted top layer were studied and the mobility of the elements was assessed. It was hoped that a combination of these approaches would provide some insight into the natural processes that occurred on this site after the initial deposition of the waste.

Materials and methods

Sampling and sample preparation

With the aim to study the degree and areal extent of pollution in the top soil a sampling grid of 5″×5″ latitude and longitude, respectively, was used. At each grid position, a centre point was located with GPS, and around this centre five subsamples of the upper 25–30 cm interval of the polluted overburden were taken with an 'edelman' drill rod. The first subsample was taken at the exact location of the central grid point, four others were taken at 5 m from this point in the four wind directions. Subsequently, these five samples were mixed and a composite sample of about 2 kg was collected in a plastic bag. The mixed samples were dried within 8 h after sampling in an oven at 60°C. After sample homogenisation and splitting, about 25 g of each sample was prepared for further chemical analysis by grinding in a Wolframcarbide mill.

Whenever iron crusts or slag materials were present on the grid points, they were also sampled and analysed. The iron crusts consist of a brown to black matrix with an earthy lustre coating and cm-sized fragments of variable colours and lustre, and their surface is brown to red coloured due to the dominance of oxidized Fe-bearing phases. The slag materials can macroscopically be divided into two types. Type I is characterized by its glassy outline and fracture surfaces. It often has a glassy black lustre with flow structures which are accentuated by spherical or ellipsoidal cavities of different sizes (sub-millimeter to a maximum of 3 cm). The latter relate to gas bubbles which became enclosed during rapid cooling of the smelt. This type of slag material possesses many features in common with volcanic glass or obsidian. The morphological characteristics are also comparable with the glassy particles that form during incineration of municipal waste, when non-combustible materials and unburned organic matter are collected in a quenching/cooling tank (Sabbas et al. 2003), the so-called municipal solid waste incinerator (MSWI) bottom ash as described by Zevenbergen et al. (1996). Type II slag material has an earthy lustre and individual mineral phases can be differentiated macroscopically. Its texture resembles volcanic rocks containing phenocrysts and rock fragments. Both slag types were sampled and their mineralogy determined.

After the initial mapping, some soil profiles below the polluted top layer were studied. Within the flat "Maatheide site", one major soil type occurs, namely a Podzol, which is typical of major parts of NE-Belgium. However, a large variation in profile development can be seen on the site, from well developed, well drained Podzols to well developed hydromorphic Podzols or weakly developed Podzols, which is characterized by a difference in the development of the spodic horizon. These profiles have been preserved to a different degree depending on their location in the site. In some places, the polluted top layer has disturbed the underlying profiles completely, and especially where the zinc smelter is located, the natural top of the profiles is absent. Elsewhere, partly or completely undisturbed Podzol profiles still exist, of which some were sampled and analysed to study the fate of the heavy metals in the subsoil with special focus on the behaviour of heavy metals in the spodic horizon.

Two examples of dry Podzols with an (E)–B_h–B_{hs}–C profile development, located below a thick (> 30 cm) layer of waste material, will be discussed here. The A_h horizon was in both cases no longer present due to the disturbance of the top layer. The C-horizon consists of gravel of the river Meuse and aeolic sands of the Quaternary age. A more detailed description of the profiles is given in Table 1. Soil profile samples were taken of all horizons in the soil profiles. These samples were dried at 60°C, sieved (< 2 mm) and stored in glass bottles for analysis.

Methods

Determination of pseudo-total element content

For the determination of the pseudo-total element content, 1 g of the samples was dissolved in a mixture of three acids, considered to reflect a total leach. For this, samples were transferred to Teflon cups, and 4 ml of hydrochloric acid 37%, 2 ml of sulphuric acid 65% and 2 ml of hydrofluoric acid 48% were added. The cups were then heated at 200°C until semi-dry and the procedure was repeated. When the samples were completely dry, 20 ml of 1N HNO_3 was added. Subsequently, the samples were heated to bring all soluble components in

Table 1 Description of soil profiles

MT 02.01: Iron-humus Podzol (Zcg) Sandy profile located next to an asphalted road. Below a waste layer of 40 cm (Anthrosol) a Podzol profile is present		MT 03.5 Iron-humus Podzol (Zcg) Podzol profile present below waste layer of 1 m thickness. Vegetation: grass. Roots are found until 50–60 cm depth	
51.1.1 Spolic anthrosol		*51.1.2 Spolic anthrosol*	
0–20 cm	More or less layered overburden containing fragments of brick, slags, etc Mixed colours: 10 YR 5/8, N1.5/0, 10 YR 7/3, main colour 10 YR 3/2 à 3/3. Surface loose, structureless. No vegetation, no roots, no soil fauna present. Structure: only packing voids	0–20 cm	Contains stones, mix of grey, ochre, black (7.5 YR 5/8 + N1.5/0). Strongly rooted. Crumby structure.
20–38 cm	Irregular layer (10 YR 6/3–6/4) with stains (7.5 YR 5/8) and grey streaks (10 YR 6/2)	20–40 cm	10 YR 1.7/1. Close root net, crumby structure. Contains stones, glass, etc.
		40–60 cm	N2/0 (metallic). Closely rooted, contains stones and glass
		60–80 cm	N2/0 (metallic). Contains many stones (bricks), slags and such like
		80–100 cm	5 PB 1.7/1. Contains many stones
Podzol (*Zcg*)		*Podzol* (*Zcg*)	
38–45 cm	E-horizon: grey (N6/0–5/0–4/0), clearly delineated horizontal boundary with waste layers above, and B-horizon below. No roots. Sandy texture, fairly friable consistence, massive structure	100–105 cm	E horizon: difficult to define, forms a transition zone between the Podzol profile and the disturbed layers on top (N3/0–2/0 + 10 YR 6/3)
45–58 cm	B_h-horizon: black (10 YR 1.7/1 à N1.5/0). Sharply delineated, horizontal boundary with the E horizon, somewhat more diffuse boundary with underlying horizons. No roots. Sandy texture, consistence fairly hard when moist but brittle upon drying, massive structure.	105–110 cm	B_h-horizon: black (N2/0 + 7.5 YR 2/3 (brown spots), compact, quite hard. Clearly separated from the layers above
58–65 cm	B_h-horizon: brown horizon (10 YR 4/6), with thin horizontal humus bands at 60–65 cm depth. Some bands run over the entire profile wall, others are shorter and interrupted. No roots. Sandy texture, consistence hard but easily disrupted when dry, massive structure.	110–115 cm	B_{hs}-horizon, divided into two sub-horizons because of gradation of dark to lighter brown. Humus bands run more or less horizontally through horizon110–112 cm: 7.5 YR 3/3 112–115 cm: 7.5 YR 3/4
65–85 cm	B_{hs}-horizon: brown horizon (10 YR 4/6) with short vertical humus bands (few cms long). Darker orange spots in pale-yellow matrix, reddish brown spots (10 YR 4/6). Large root passage at 65–70 cm	115–125 cm	Lighter coloured layer with humus bands. Matrix pale yellow, darker orange stains occur (10 YR 5/6 (à 7.5 YR). Contains pieces of wood
85–125 cm	C-horizon: Sand has a lighter colour, is less hard. Yellow spots (10 YR 7/6 à 6/6) are interchanged with white lenses (2.5 Y 7/2). Iron rich aggregates containing small pebbles, iron rich nodules	125–165 cm	Spotted horizon. Matrix pale colour (10 YR 7/6) with darker orange stains that occur diffusely (7.5 YR 5/8)
		165 cm	Well rounded pebbles, possible pebbles of the Meuse terraces are present as a layer at this depth, some larger than 10 cm diameter

The colours have been determined with a Munsell Colour Chart (1997) in field-moist condition

suspension and filtered on Whatman 43 filters. The insoluble residue (IR) was determined as the mass percentage of the samples remaining on the filters (after drying at 60°C). Based on SEM-EDX as well as XRD analysis, the latter consists nearly exclusively of quartz phases. An international standard (Montana soil SRM 2710) was added as a reference, while about 10% of the samples were analysed in duplicate to determine the reproducibility of the analyses. For the 144 grid samples, Ca, Cd, Co, Cu, Fe, Mg, Mn, Ni, Pb and Zn were measured by Flame A.A.S. (F.A.A.S.). Analytical precision was better than 10% for all elements at concentrations three times the detection limit (1–2 mg/kg level). Only Cd concentrations were often close to the detection limit of 0.5 mg/kg and precision was, therefore, low in this case (Adriaensen et al. 2000).

In the soil profile samples, major elements (Fe, Al, Ca) were measured with an Atomic Absorption Spectrometer (AAS, Varian Techtron AA6), while trace elements (As, Cd, Co, Cr, Cu, Mn, Ni, Pb, Zn) were analysed by an inductively coupled plasma-mass Spectrometer (ICP-MS, HP 4500). Prior to the determination of the trace element content, the samples were diluted with 5% HNO_3 (ultra pure) and an Indium (In) internal standard was added to correct for shifts in sensitivity. All ICP-MS measurements were repeated three times, with standard deviations between measurements well below 5%.

Soil characteristics

For pH measurement of the grid samples, 10 g of soil sample was mixed with 25 ml of a 1 M KCl solution and shaken for 2 h. After sedimentation for at least 30 min, the pH was measured with a microprocessed pH meter. Soil acidity (pH) of the soil profile samples was measured in a suspension of soil and water, with a soil to water ratio of 1:2.5, which was stirred for 20 min. A Hamilton Single Pore® Ag/AgCl electrode, stored in 3 M KCl, was used for the measurement after calibration against buffers of pH 4 and 7. Organic carbon content was determined with the Walkley and Black titration method (Nelson and Sommers 1982).

Table 2 Extraction procedure modified from Tessier et al. (1979)

Extraction method	Dissolved fraction
Distilled water	Water soluble
NH_4Ac (1 M), pH 7.2	Ammonium exchangeable
NaAs (1 M), pH 5, acidified with HOAc	Acid soluble
$NH_2OH.HCl$ (0.1 M), HNO_3 (0.01 M), pH 2	Easily reducible
NH_4Ox (0.2 M), oxalic acid (0.2 M), pH 3	Reducible
30% H_2O_2, HNO_3, pH 2 → NH_4Ac (1M)	Oxidizable
HNO_{3conc}, HCl_{conc}, HF_{conc}	Residual

Mineralogy

A mineralogical study of the top soil samples was carried out by microscopical techniques as well as by XRD analysis. The results of the different methods were combined to get an overview of the mineralogy of the top soil constituents.

The 63–250 μm fraction of selected crushed samples was separated into a magnetic and non-magnetic fraction. Since the non-magnetic fraction contained large amounts of quartz, this fraction was further fractionated based on density separation, by bromoform ($\rho = 2.89$ g/cm^3). XRD analysis was then carried out on the different fractions. Individual topsoil grains and fragments of slag material and iron crusts were also examined by Scanning Electron Microscopy (SEM) and analysed by EDX. After binocular examination of anomalous samples, interesting soil phases were handpicked and polished for reflected light microscopical analysis. Interesting phases from iron crusts and slag material were also selected for further examination.

This method, in combination with XRD, allowed the determination of the mineralogical composition of individual grains. Additionally, information on the alteration of certain compounds and the structure and morphology of mineral phases was collected.

Some of the samples selected for SEM analysis were also analysed by microprobe. The elements Zn, As, Si and Al were analysed by a TAP detector, S, Pb and Cd by a PET detector and Fe and Cu with a LiF detector. Analyses were made by 15 kV and 20 nA.

Mobility

Ten composite topsoil samples of different origin and chemical composition and one crushed iron crust sample were characterized by a sequential extraction carried out according to a modified extraction scheme based on Tessier et al. (1979). This analytical procedure, which is given in Table 2, involves the partitioning of the elements Cd, Cu, Fe, Mn, Pb and Zn into six fractions, supposedly the water soluble, cation exchangeable, carbonate-bound, Mn-oxide bound, Fe-oxide bound, organic matter/sulphide-bound and residual fraction. However, since sequential extractions are known to suffer from non-selectivity and non-specificity (Tack and Verloo 1995; Xiao-Quan and Bin 1993) these fractions are operationally defined, and most likely do not correspond entirely to the chemical pools they are supposed to represent. Therefore, the extracted fractions will be referred to below in function of the used chemical extractants, i.e. water soluble, ammonium exchangeable, acid soluble, easily reducible, reducible, oxidizable and residual (three acid) fraction.

The mobility of heavy metals in the spodic horizons of the profiles was assessed by single extractions with

$CaCl_2$ 0.01 M, EDTA 0.05 M and acetic acid 0.43 M. The extraction with calcium chloride is supposed to give the bio-available fraction of trace elements, since this reagent matches the soil solution with respect to pH, concentration and composition (Houba et al. 1996). Choosing this reagent entails the possibility of enhanced cadmium mobilization, since Cd forms soluble complexes with Cl^- (McLean and Bledsoe 1992). The extraction with EDTA 0.05 M gives an idea of the fraction of trace elements bound to complexants (such as humic acids) while the acetic acid extraction simulates acidification. All extractions were performed in triplicate according to the recommendations of the BCR (Community Bureau of Reference, now the Measurements and Testing Programme of the European Commission) (Quevauviller et al. 1997). For all extractions, blanks were included to check for possible contamination in the lab, and reference material CRM 483 was analysed to evaluate the extraction effectiveness, since for this standard certified values for Cd, Cu, Ni, Pb and Zn are available. For the $CaCl_2$ extraction, 2 g of soil and 20.0 ml of $CaCl_2$ (0.01 M) were brought into a 50 ml centrifuge tube and shaken for 3 h on a reciprocating shaker. For the extraction with EDTA, 2 g of soil sample and 20 ml of EDTA 0.05 M were brought in a 50 ml centrifuge tube and shaken on a reciprocating shaker for 1 h. The acetic acid extraction was performed by adding 40 ml of 0.43 M acetic acid to 1 g of soil sample in a 50 ml centrifuge tube and shaking this mixture overnight for 16 h. After shaking, all the samples were centrifuged for 10 min at 3,000 rpm and the solutions filtered over a 0.45 µm filter. In the $CaCl_2$ extracts, the pH was also measured. The solutions were measured with ICP-MS within a few days after the extractions. Recovery rates for the CRM 483 were generally very good, with deviations below 10% of the certified value. For Pb, the recovery rates were less satisfactory for the EDTA (72%) and CH_3COOH (64%) extraction. In the $CaCl_2$ extraction Cu (132%) and Zn (126%) were overestimated.

One sample, namely the spodic horizon of soil profile MT03.5, was subjected to a pH_{stat} analysis, to study heavy metal mobility in function of pH. For this analysis, five subsamples of 80 g each were transferred to a glass flask, and 800 ml of deionised water was added. The samples were then maintained at a fixed pH for 96 h under continuous shaking. With the TitroWico® titrator, the pH was constantly monitored and when necessary corrected by either HNO_3 (nitric acid) or NaOH (sodium hydroxide). This experiment also allows for the ANC (acid neutralisation capacity) and BNC (base neutralisation capacity) to be calculated from the amount of acid or base added. The chosen pH values were 2, 3, 5 and 8. In one subsample, the pH was continuously measured, but no titrans was added (natural pH).

Results

Grid samples

Elemental analysis of polluted topsoil around the Maatheide smelter

The areal distribution pattern is quite similar for all elements, with very high concentrations for most heavy metals (e.g. average values of 23 mg/kg Cd and 4,232 mg/kg Zn, maximum values of 319 and 56,385 mg/kg respectively). As an example, the distribution patterns of Zn and Cd on the site are shown (Figs. 2, 3). The entire data set can be requested from the authors. The soil pH is high at locations with high contents of heavy metal bearing industrial waste (Fig. 4). Element variation between samples relates to differences in quartz, organic matter, but especially slag content. Naturally, the highest concentrations are found on the former smelter site, as well as in northeastern direction, i.e. in the downwind direction of the latter. Furthermore, elevated concentrations occur at the northern side of the zinc smelter, where fine-grained ashes and slag material are present and in an area south of the latter, where ceramic pipes containing variable amounts of metal-bearing ashes were dumped. In these pipes ore material was smelted and zinc-containing vapours migrated through the pipes. The degree of pollution diminishes to the east of the site, where no industrial activities have taken place. However, the concentrations are still high (Cd mostly over 1 mg/kg, Zn mostly higher than 100 mg/kg) compared to background values, such as determined for example by Bosmans and Paenhuys (1980) (5–15 mg/kg Zn, 0.15–0.45 mg/kg Cd, 15–45 mg/kg Pb and 1.5–4.5 mg/kg Cu for forest soils) or in the pristine layers of overbank sediments in northern Belgium (62 ± 152 mg/kg Zn, 0.7 ± 0.4 mg/kg Cd, 37 ± 111 mg/kg Pb and 10 ± 17 mg/kg Cu) (Swennen et al. 1998). The high concentrations are explained by the dumping of waste material as well as atmospherical pollution.

Clearly, large variations in heavy metal contents are found, with locally very high concentrations for Zn, Pb, Cu and Cd. According to the Flemish law for Soil Remediation (Vlarebo, Anonymous 1996) the maximum allowed concentration for soils on industrial sites is 30 mg/kg for Cd, 800 mg/kg for Cu, 2,500 mg/kg for Pb and 3,000 mg/kg for Zn. However, these are the values for a standard soil, with 10% of clay and 2% of organic matter. According to the Aardewerk database (Librecht et al. 2002), the soil types occurring on this site have an average clay content of only 1–2, and 2% organic carbon (which equals 3.4% organic matter when using the standard conversion factor of 1.72). The adapted maximum concentrations for a soil with 1.5% clay and 3.5% organic matter are 23.3 mg/kg for Cd, 680 mg/kg for

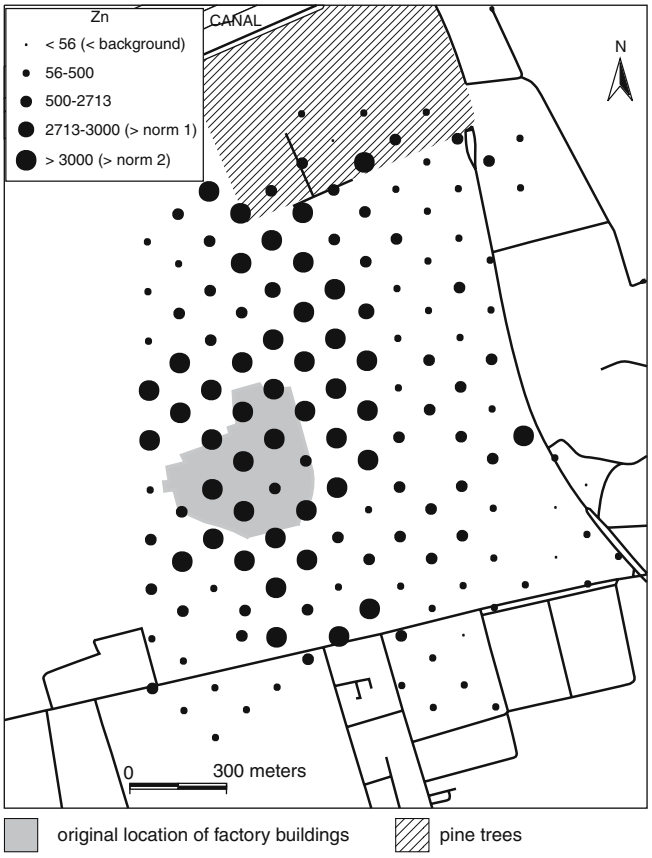

Fig. 2 Distribution pattern of Zn on the site. Background, norm 1 and norm 2 refer to the background and reference values according to the Vlarebo (Anonymous 1996) (see Elemental analysis of polluted topsoil around the Maatheide smelter). Norm 1 is the adapted reference value, norm 2 is the reference value for a standard soil. Concentrations are given in mg/kg

Fig. 3 Distribution pattern of Cd on the site. Background, norm 1 and norm 2 refer to the background and reference values according to the Vlarebo (Anonymous 1996) (see Elemental analysis of polluted topsoil around the Maatheide smelter). Norm 1 is the adapted reference value, norm 2 is the reference value for a standard soil. Concentrations are given in mg/kg

Cu, 2,555 mg/kg for Pb and 2,713 mg/kg for Zn, and are exceeded in 31% of the studied top soil samples for Zn, in 20% for Cd and in about 6% for Pb and 8% for Cu. These results were one of the reasons why the site was remediated in 2004. The adapted background concentrations in these soils, according to the Vlarebo, are 0.6 mg/kg Cd, 14.5 mg/kg Cu, 41 mg/kg Pb and 56 mg/kg Zn. On the maps in Figs. 2 and 3, the size classes of the markers are partially based on these background and remediation values.

Mineralogy

XRD analyses of the top soil magnetic fraction revealed that goethite (α-FeO(OH)), hematite (Fe_2O_3), magnetite (Fe_3O_4) and lepidocrocite (γ-FeO(OH)) are omnipresent. Other identified Fe-containing phases are strengite ($(Fe,Al)PO_4{\cdot}2H_2O$), franklinite ($(Zn,Fe,Mn)(Fe,Mn)_2O_4$), heterosite ($(Fe,Mn)PO_4$) and cohenite (FeC). In the magnetic fraction small amounts of non-Fe-containing phases were also present such as enargite (Cu_3AsS_4), alabandite (MnS), pyrolusite (β-MnO_2), ramsdellite (MnO_2) and pyrochroite ($Mn(OH)_2$). They most likely occur as intergrown phases within the magnetic phases.

In the low density non-magnetic fraction, quartz was the dominant mineral, with small amounts of rutile (TiO_2), gypsum ($CaSO_4{\cdot}2H_2O$) and calcite ($CaCO_3$). Hematite was also found, which can be explained by the fact that it occurs as coatings around quartz grains.

In the high density non-magnetic fraction, a number of zinc phases were identified such as zincite (ZnO), willemite ($ZnSiO_4$), hemimorphite ($Zn_4(Si_2O_7)(OH)_2{\cdot}H_2O$), and native Zn. These mineral phases originate from the ore or the ore processing. Apart from these Zn phases, other heavy metal-bearing phases have been identified by XRD (Table 3). Since they have different origins, they are divided accordingly in different classes.

Minerals of class I are considered to represent ore minerals, mostly sulphides and gangue minerals. Class II represents secondary minerals and mineral phases which

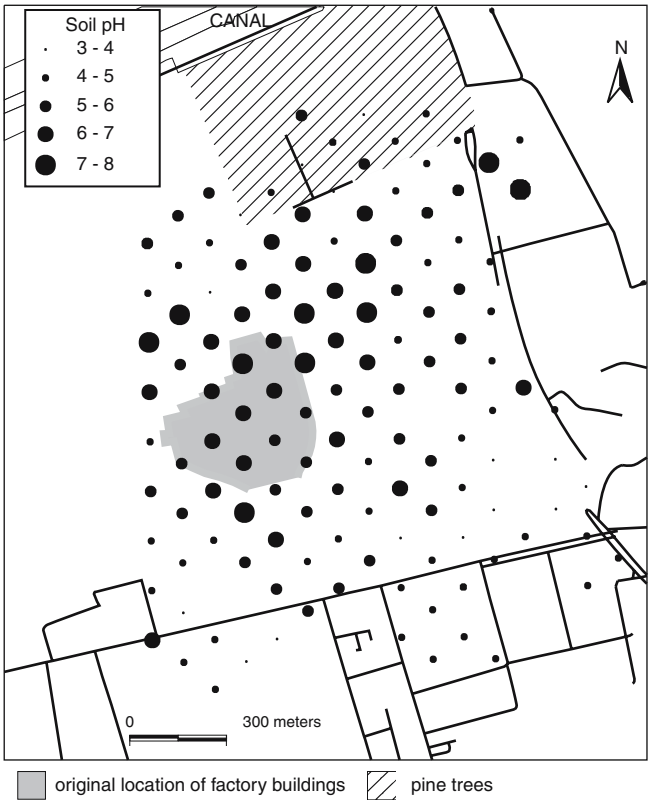

Fig. 4 Distribution pattern of pH on the site

occur in the oxidized zone of ore bodies, but it is more likely that they formed due to 'in situ' alteration on the Maatheide site. Class III represents metallurgical phases relating to the smelting process. Class IV contains minerals and phases that are difficult to place in one of the former classes. The origin of some minerals such as sphalerite (class I) and cohenite (class III) is rather certain, but Table 3 also contains a number of minerals such as goethite (class II and III) and zincite (class I and III) with an uncertain origin. Quartz, which is the main component of the parent material is, of course, omnipresent.

Most samples of type I slag material consist of very homogenous, amorphous phases containing S, Si, and Al as major elements. X-ray diffractograms of these samples show no distinct pattern, with typically very high background signals. In general, this material possesses no characteristic diffraction patterns. In some cases, cristoballite (SiO_2) and ringwoodite [$(Mg,Fe)_2SiO_4$] have been identified. In these samples, exsolution textures have been observed. SEM-EDX analysis shows that Fe occurs in variable amounts and traces of Ca, K, Zn and Ti are often detected. Exsolution element patterns were observed and analysed by microprobe. The dominant phase or matrix consists of an Fe-rich (average 78.2 g/kg) material with Si (average 281.6 g/kg), Zn (average 40 g/kg) and Pb (average 9 g/kg). The exsolution phase contains on average more Si (337 g/kg) and Zn (72.4 g/kg) but less Fe (13.5 g/kg).

The matrix of type II-slag materials consists of a mineralogically non-identified Al–Si–S–K-phase with traces of Ca, Ti and Mn. Within this matrix a number of minerals have been identified such as cuprite (Cu_2O), troilite (FeS), pyrite (FeS_2) and franklinite ($ZnFe_2O_4$) next to secondary phases such as akaganeite (β-FeO(OH)), goethite (α-FeO(OH)) and lepidocrocite (γ-FeO(OH)). In some of these samples, reaction rims were recognized indicating the different degrees of weathering of unstable phases.

Sequential extraction of ten topsoil samples

Figure 5 shows the results of the sequential extraction for Zn, Cd, Pb and Cu. The samples have been sorted by increasing pseudo-total element content of Zn. These results allow to deduce whether the heavy metals in the different samples have a similar or different fractionation. In Table 4, metal contents of the selected samples are given as well as a brief description of distinguishing features. Fe12 is the iron crust sample and will be discussed separately. By combining these results with the data from the mineralogical analysis, the different chemical forms under which the metals are present can be inferred.

Generally, it can be seen that samples with a similar total element content behave more or less in a similar way. For Zn, the relative contribution of the residual fraction seems to increase as the total element content increases. This fraction is in principle mainly related to silicates and the glass fraction and thus considered to be immobile. Petrographical and SEM-EDX analysis confirmed the omnipresence of Zn-bearing glass components. Other important fractions for Zn are the acid soluble and reducible fractions, and to a lesser extent oxidizable fractions. Zinc carbonates and sulphides were indeed recognized by XRD, and SEM-EDX results showed that Zn is often present in Fe-oxi/hydroxides or even that Zn-oxides are intergrown with different Fe-oxi/hydroxides and illite. However, the amount of Zn that is bound to the reducible fractions (supposedly Fe/Mn oxi/hydroxides or amorphous Fe-oxi/hydroxides) does not seem directly related to the Fe content of the samples. For example, no significant difference can be noted between G70 (100 g/kg Fe) and G81 (4 g/kg Fe), while samples G131 and G191 contain far less Fe than G12, G49 or G69. Probably not all Fe is present as reducible Fe oxi/hydroxides. For some samples, the ammonium exchangeable fraction is also significant, and shows that an important quantity of Zn is easily mobilized.

Table 3 Minerals identified by XRD (X-ray diffractometry)

Class I	Class II		Class III	Class IV
Alabandite[a]	Goethite[a]	Arthurite	Enstatite	Chamosite
Arsenopyrite	Hematite[a]	Frondelite	Cohenite	Hydroxyapophyllite
Bornite	Hydrozincite[a]	Dufrenite	Schreibersite	Saponite
Carrolite	Franklinite[a]	Drugmanite	Fayalite	Saponite (Al)
Chalcopyrite	Heterogenite	Barbosalite	Zinc	Calcite[a]
Chalcosite	Brucite	Collinsite (Zn)		
Mackinawite	Crichtonite	Cornetite		
Marcassite	Ferrihydrite[a]	Giniite		
Pyrite	Cuprite[a]	Heterosite		
Pyrrhotite[a]	Spertinite	Strengite		
Smythite	Theophrasite	Triploïdite		
Sphalerite	Wuestite	Whitmoreite		
Violarite	Zincite[a]	Wolfeite		
Troilite	Plattnerite	Sarcopside		
	Ramsdellite[a]	Scholzite		
Enargite	Lepidocrite	Jungite		
Tennantite	Manganite	Reddingite		
Tetraetaenite	Jeanbandyite	Koninckite		
Tetrahedrite		Magniotriplite		
Loellingite	Anglesite			
	Bianchite	Rosasite, Zn[a]		
Magnetite[a]	Beudantite	Otavite		
Pyrolusite	Chalcocyanite	Malachite[a]		
Rutile[a]	Eugsterite	Plumbonacrite		
	Goslarite			
Dolomite[a]	Ilesite	Nealite		
Ankerite	Diadochite	Hemimorphite		
Phlogopite	Larnakite	Diaboleite		
Vermiculite	Linarite	Ferrimolybdite		
Biotite	Melanterite	Crocoite		
Scorzalite	Leadhillite			

[a]Minerals frequently observed

For both Cd and Pb, the acid soluble fraction is significant. The corresponding carbonates were found to be present, and calculations with MINTEQA2 4.02 (Allison et al. 1991) showed that these carbonates can dissolve at the pH of the extraction. Pb seems however to be less mobile, since the residual fraction is significantly larger than for Cd, where the ammonium exchangeable fraction reaches up to 30–35%. In general, it can be said that Cd is more mobile than the other elements, which has often been reported in literature (Mench et al. 1994).

Finally, Cu seems to be largely bound to the reducible and oxidizable fractions. Several Cu sulphides were identified by XRD, as well as oxi/hydroxides containing Cu. Although malachite was frequently encountered, and dissolves at the pH of the extraction (according to calculations with MINTEQA2 4.02), the amount of Cu found in the acid soluble fraction is quite limited. Compared to Zn and Pb, significantly larger amounts of Cu are found in the reducible fraction (supposed to represent Fe/Mn oxides or amorphous Fe-oxi/hydroxides). This could be due to the fact that Cu^{2+} adsorbs on goethite at a lower pH, i.e. at pH 5–6 than Zn^{2+}, Co^{2+} and Cd^{2+}, which adsorb at pH 7–8 (Spark et al. 1995; Agbenin and Olojo 2004). This makes Cu adsorption more likely in these naturally acid soils. Whether this is also the case here, where pH values in the topsoil vary around 7 due to the presence of waste material, is unknown. Agbenin and Olojo (2004) also found that when Zn and Cd are in competition for binding sites in soils, reactions with organic matter and amorphous oxides are the major controls on Cu while Zn might be largely sorbed by cation exchange reaction, and that metal binding sites in amorphous hydrous oxides and organic matter were more selective for Cu than Zn.

In general, significant portions of the heavy metals can thus be mobilized under changing pH or redox conditions, and pose a threat to human health and the environment. Another observation is that some samples exhibit similar behaviour even though their pseudo-total heavy metal content differs widely, while others with similar contents behave very differently. This suggests that pseudo-total element content, as could be expected, is not the only determining factor, but speciation (i.e. mineralogy) is also important. For all the elements, the sample treated with beringite (G80) does not seem to differ markedly from the other samples. This lack of difference in speciation between unremediated soils and soils treated with beringite was also observed in another

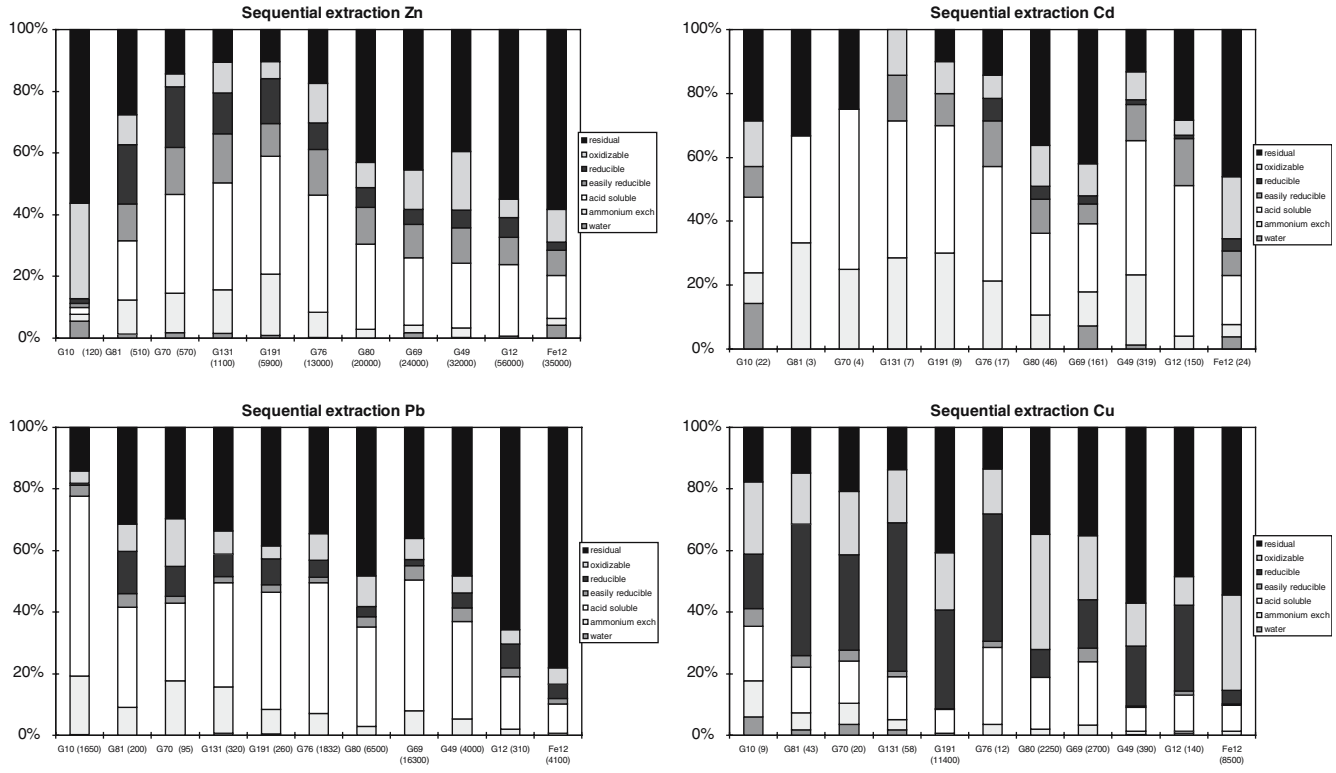

Fig. 5 Results of the sequential extraction. Total concentrations (in mg/kg) are shown between brackets after the sample name. The samples are sorted according to increasing Zn content

study on this site, using single extractions and XAFS (D. L. Sparks 2005, personal communication).

Soil profiles

Element content

In the sandy soil profiles, only Cd and Zn are found in significant amounts, therefore, the discussion will be mainly limited to these elements. Figure 6 presents the distribution of Cd, Zn, Al, Fe, pH and organic carbon with depth. In the anthropogenically disturbed overburden layers, concentrations of Zn vary from 336–16,500 mg/kg for MT02.1 and 585–31,175 mg/kg for MT03.5. Cd concentrations range from 9 to 51 mg/kg in MT02.1 and 10 to 153 mg/kg in MT03.5. Although the concentrations below the disturbed layers are much lower than in the top soil, there is a clear enrichment of heavy metals in the spodic horizon (Fig. 6). In MT02.1, 21–48 mg/kg Cd and 600–1,800 mg/kg Zn are found in the B_h, for MT03.5 this is 20–25 mg/kg Cd and 600 mg/kg Zn. The concentrations of Cd and Zn also seem to follow the same trend as organic carbon (4–6% in the spodic horizon). The concentrations of Al and Fe are fairly low, and the relationship with the heavy metals is unclear. In MT03.5, an increase in Al and Fe concen-

Table 4 Properties of samples selected for sequential extraction

Sample	Fe (g/kg)	Zn (g/kg)	Pb (g/kg)	Cu (mg/kg)	Cd (mg/kg)	pH_{soil}	Comments
G10	0.4	0.12	1.7	9	22	4.2	High gypsum content combined with low pH
G12	28	56	0.31	140	150	7.9	High zinc content
G49	39	32	4	390	319	6.2	High cadmium content
G69	48	24	16	2,700	161	6.0	High lead content
G70	99	0.57	0.1	20	4	5.1	High iron content
G76	47	13	0.079	12	3	6.1	On top of iron crust
G80	74	20	6.5	2,250	46	7.0	Treated with beringite
G81	4	0.51	0.2	43	3	5.6	Relatively low concentrations of heavy metals
G131	5.9	1.1	0.32	58	7	5.8	Relatively low concentrations of heavy metals
G191	7.8	5.9	2.6	11,400	9	5.0	High copper content
Fe12	25	35	4.1	8,500	24		Iron crust

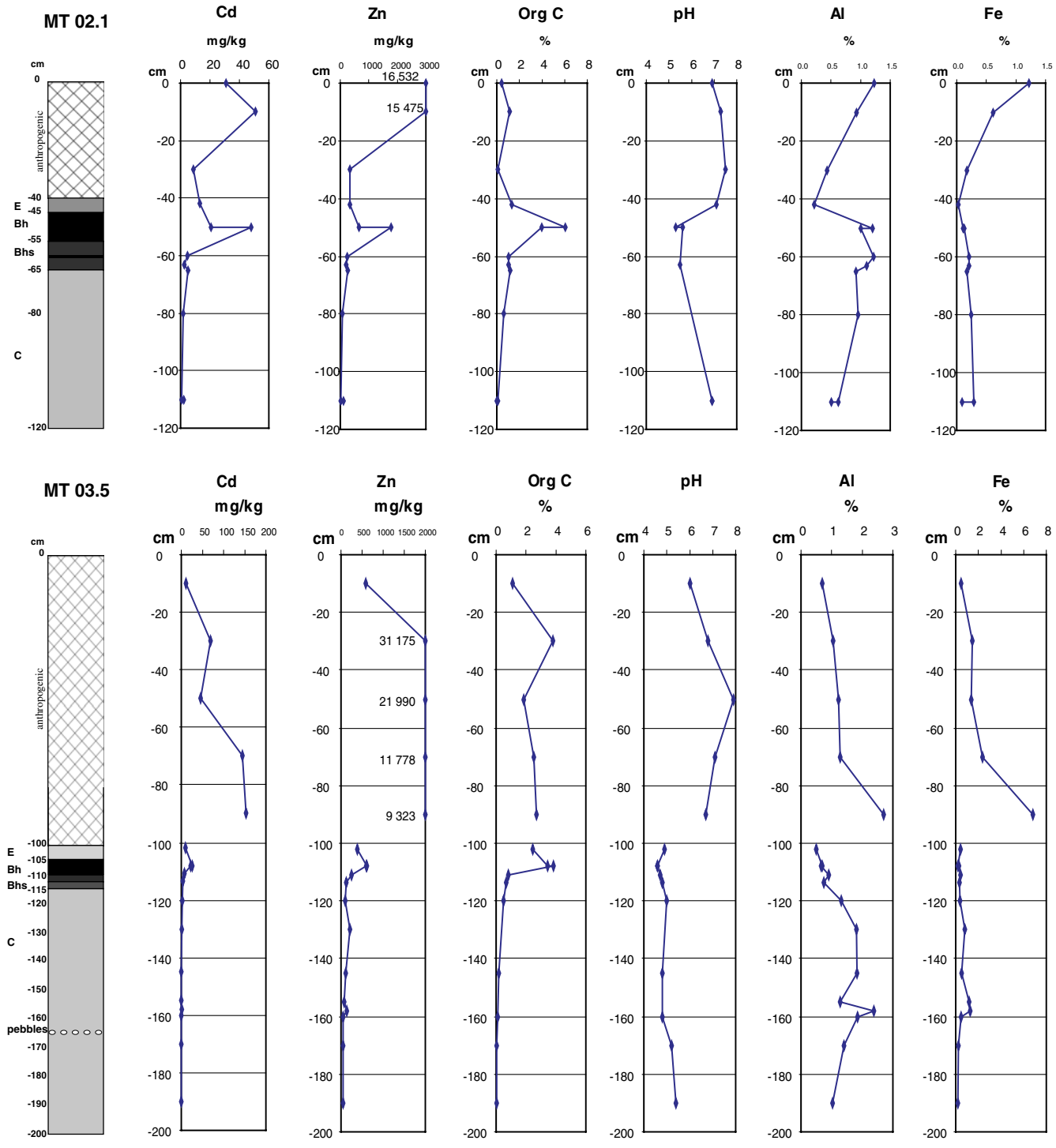

Fig. 6 Distribution pattern of Cd, Zn, organic carbon (Org C), pH, Al and Fe along the profiles MT 02.1 and MT 03.5. *E* eluvial horizon, *Bh* spodic horizon enriched in organic matter, *Bhs* spodic horizon enriched in organic matter and iron oxi/hydroxides, *C* transition zone to parent material

trations at 150–160 cm depth coincides with a slight increase in Cd and Zn content. In the undisturbed soil horizons, pH is about 4–5, while this is much higher in the overburden (pH = 7–8). In other profiles (results not

Table 5 Results of single extractions

	MT02.1 B_h			
	Cu	Zn	Cd	Pb
MT02LH005				
$CaCl_2$	dl	514 ± 26 (29%)	10.34 ± 0.25 (21%)	dl
EDTA	dl	1,375 ± 17 (78%)	41.4 ± 0.9 (86%)	1.83 ± 0.05 (31%)
CH_3COOH	dl	1,104 ± 33 (62%)	30.4 ± 0.6 (63%)	dl
Total conc.	dl	1,773	48	6
MT02LH006				
$CaCl_2$	dl	155 ± 8.4 (24%)	3.17 ± 0.14 (15%)	dl
EDTA	dl	547 ± 19 (83%)	17.9 ± 0.6 (86%)	2.98 ± 0.07 (40%)
CH_3COOH	0.02 ± 0.02	456 ± 40 (69%)	11.7 ± 0.7 (56%)	dl
Total conc	dl	656	21	7
	MT03.5 B_h			
	Cu	Zn	Cd	Pb
MT02LH027				
$CaCl_2$	2.39 ± 0.05 (1.5%)	305 ± 14 (51%)	9.10 ± 0.33 (41%)	dl
EDTA	179 ± 5 (111%)	479 ± 15 (80%)	21.0 ± 0.6 (94%)	4.94 ± 0.15 (45%)
CH_3COOH	35 ± 3 (22%)	427 ± 20 (72%)	14.3 ± 0.1 (64%)	0.11 ± 0.07 (1%)
Total conc.	161	596	22	11
MT02LH028				
$CaCl_2$	3.50 ± 0.08 (3%)	369 ± 26 (60%)	13.1 ± 0.7 (51%)	dl
EDTA	154 ± 5 (118%)	515 ± 25 (83%)	24.3 ± 1.2 (95%)	5.85 ± 0.19 (52%)
CH_3COOH	40.9 ± 0.5 (31%)	489 ± 21 (79%)	19.8 ± 0.7 (77%)	0.49 ± 0.07 (4%)
Total conc.	131	618	26	11

Concentrations are given in mg/kg, mean of three repetitions ± standard deviation. Percentage of total concentration is shown between brackets, *dl* below detection limit

shown) where no clear spodic horizon was present, no accumulation of heavy metals occurred.

Mobility

Table 5 shows the results of the single extractions, performed on the samples of the spodic horizons of both Podzol profiles. For the samples of MT02.1, only Cd and Zn will be discussed, since Cu and Pb were not found in significant amounts in this profile. Both Cd and Zn are fairly mobile, considering the relatively high amounts released with the $CaCl_2$ extraction (Cd 15–21%, Zn 24–29%). For Cd, this means that concentrations of up to 10 μg/l could be present in the pore water (under the assumption that $CaCl_2$ simulates pore water), while the Vlarem norm reference value is 5 μg/l for groundwater (Anonymous 1996). About 80% of the heavy metals are released with EDTA, which suggests that these elements are bound to the organic matter (complexing agent). Upon acidification, 60% of the elements are released.

For MT03.5, generally the same observations are valid, but Cd and Zn are even more mobile since 40–50% of the elements are released in the $CaCl_2$ extraction. Although the concentrations of Pb and Cu are still not very high in these soils, it can be seen that Cu also seems to be largely bound to the organic matter, and is, therefore, completely released in the EDTA step.

In Fig. 7, the end concentrations of the pH_{stat} experiment are given. The final pH of the sample where the pH was measured, but not adjusted by addition of an acid or base, was 3.6. The natural pH of the spodic horizon is thus quite low. However, it can be seen from Fig. 7 that a slight decrease in pH (from 3.6 to 3) already causes a significant increase in Zn and Cd mobilization. The ANC, calculated from the amount of acid necessary to reach the desired pH, was 27.5 meq/kg for reaching pH 3, and 103 meq/kg for reaching pH 2. Due to this low buffering capacity, a pH decrease to pH 3 or lower seems realistic in these soils. At the natural pH, the release is quite limited, and increasing the pH to 6 or 8 leads to almost complete immobilisation of Cd and Zn. For Cu, the behaviour is different. Here, both an increase and a decrease in pH stimulate mobilization. The concentrations of Pb in this sample were very low, and fell below the detection limit of the ICP-MS.

Iron crusts

As mentioned before, the iron crusts are probably formed by dissolution and subsequent reprecipitation of

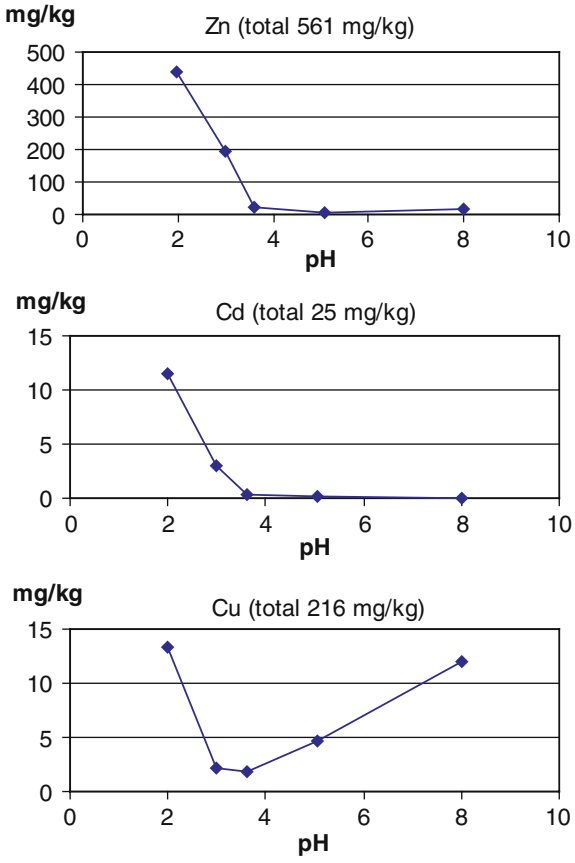

Fig. 7 Results of pH_{stat} experiment, release of Zn, Cd and Cu in function of pH. *Total* total element content

iron oxi/hydroxides and crushed slag material, and occur mainly on former roads on the site.

Mineralogy

After magnetic separation, XRD-analysis revealed that apart from quartz, sulphides of the different heavy metal species and Fe-oxi/hydroxides make up the bulk of the iron crusts. The iron oxi/hydroxides are volumetrically the most important mineral group, consisting mainly of goethite [α-FeO(OH)], often with a colloform outline, and hematite (Fe_2O_3). Franklinite ($ZnFe_2O_4$) and akageneite [β-FeO(OH)] have also been identified.

Sphalerite (ZnS), pyrrhotite (FeS), bornite (Cu_5FeS_4), digenite (Cu_9S_5), enargite (As_3AsS_4) and pyrite (FeS_2) were identified; however, their occurrence is limited. Zn and Fe were also present as native element species and as oxides such as zincite (ZnO), tenorite (CuO), massicot (PbO) and in more complex structures such as gahnite ($ZnAl_2O_4$) and crocoite ($PbCrO_4$).

Secondary phases in relation to the alteration and weathering of the sulphides such as gypsum ($CaSO_4$), anhydrite ($CaSO_4{\cdot}2H_2O$) and iron phosphates such as heterosite [(Fe, Mn)PO_4] and giinite [$FeFe_4(PO_4)_4(OH)_2{\cdot}2H_2O$] are also common. Phosphates within these phases may have been derived from the compost and municipal waste that were dumped on the site.

EDX analysis of goethite, which is present in nearly all of the crust samples, revealed the presence of high (percentage level) Zn, Ca and Cu concentrations. Minor amounts of Si, Al and S were also detected, but these elements, as well as Ca, can relate to non-Fe-oxi/hydroxide impurities. Microprobe analysis shows that goethite, which on average contains almost 600 g/kg Fe, also contains significant amounts of Zn (on average 11.1 g/kg), S (on average 1.6 g/kg) and Si (on average 3.7 g/kg). With microprobe, 71.4 g/kg Pb was detected in sphalerite (482.5 g/kg Zn and 247.2 g/kg S). This mineral also contains Si (35 g/kg), Al (6.3 g/kg) and Fe (13.4 g/kg). It, therefore, seems likely that the analysed sphalerite is a replacing phase with relict clay components.

SEM-EDX analysis of the surface of slag fragments very often shows a coating of illite around slag particles. These clay phases also contain high concentrations of metals such as Fe, Zn and Cu, and are believed to originate from the weathering of slag material that, as mentioned earlier, can be compared with MSWI bottom ash, wherein evidence of neoformation of well-ordered clay (illite) from glasses was found after 12 years of natural weathering (Zevenbergen et al. 1996). Glassy phases were also detected in the iron crust. EDX-analysis shows that these amorphous phases contain high concentrations (percent-level) of S, Zn and Fe and smaller amounts of Si, Ti, Cr, Cu, As and Cl.

Elemental composition based on bulk iron crusts

Heavy metal and elemental composition of bulk iron crusts is given in Table 6. The most abundant element is clearly Fe, with average values varying around 190 g/kg. This value is lower than expected, but this can be explained by the presence of glassy phases that cause a dilution effect (Fig. 8). Zn is also a major element, reaching amounts on average of 39 g/kg, which is more than found in the topsoil samples. Contrary to the topsoil samples, where the non parametric Spearman Rank R test ($n = 143$, $p > 0.05$) showed high correlation coefficients between the analysed elements and with the soil pH (which was also apparent in the distribution patterns of the elements), not all the elements show a significant correlation in the iron crust. Significantly positive values exist between Cd–Zn–Pb, Fe–Mn, Ca–Mg and relate to the pollution source of the heavy metals. Substitution of Ca by Mg in carbonates such as calcite and dolomite, explains the Ca–Mg relationship ($r = 0.90$). Especially, the concentrations of Fe and Zn

Table 6 Elemental composition of iron crust ($n = 19$)

Element	Mean	Min.	Max.	σ
As	573	347	907	237
Ca	13,508	1,700	315,715	9,740
Cd	26	10	49	12
Co	245	28	518	130
Cu	9,162	1,194	15,280	2,947
Fe	189,994	30,790	300,715	61,458
Mg	4,311	541	10,701	3,526
Mn	6,588	1,287	9,193	2,180
Ni	231	33	1,727	367
Pb	3,286	646	9,277	2,042
Zn	39,019	3,952	77,604	19,482

Concentrations are given in mg/kg

are remarkably higher in the iron crust than in the topsoil, with a Fe/Zn ratio of 5 versus a ratio of 3.5 in soil samples. This could be explained by the fact that iron crusts form out of Zn-ashes containing a lot of goethite. Those ashes are a byproduct of the smelting process.

Sequential extraction

The result of the sequential extraction of a representative iron crust sample (Fe12) is given in Fig. 5 (for Zn, Cd, Pb and Cu). The fractionation is rather similar for all analysed heavy metals, with some minor deviations such as: for Cu the reducible fraction is smaller, and the oxidizable fraction larger than for the other elements, for Cd the non-residual fraction is larger than for Zn, Cu and especially Pb where the residual fraction is larger than for the other elements. For all analysed elements, the largest amount is released in the last extraction step, i.e. the residual fraction, and thus is most likely related to amorphous glass phases. Petrographical examination of the iron crust shows that minute fragments of slag material are indeed incorporated in the iron crust, as well as in the glassy matrix (Fig. 8). Surprisingly, only some 10% is released in the reducible step, which is supposed to represent Fe oxi/hydroxides. Overall, the non-residual fraction of the iron crust sample is smaller than that of the topsoil samples.

Cd, Cu, Pb and Zn are also released in the acid-soluble and oxidizable fractions (15 and 19% for Cd, 8 and 31% for Cu, 10 and 5% for Pb, and 14 and 11% for Zn respectively). Data derived from XRD analysis as well as optical microscopy testify that bornite, galena and sphalerite are present in the iron crust, while EDX analysis showed that sphalerite contained heavy metals such as Ni, Cu and As. The oxidizable fraction, therefore, seems to reflect these sulphides. Some of the Pb and Zn released in the sulphide-related fraction can be bound in iron sulphides, whose presence is also confirmed by XRD- and SEM-EDX analyses. Microprobe analysis of Fe–sulphides shows that these mineral phases can contain up to 71.4 g/kg Pb and 0.4 g/kg Zn.

Discussion

After the industrial activities on this site were discontinued, the slag material was spread out over the entire site, together with other waste materials, and the unstable mineral phases present in this slag material released heavy metals upon weathering. As a result, the soil was polluted with heavy metals (with concentrations reaching up to percentage level) and vegetative growth was impeded over a large area, more severely than anticipated. The recalculated remediation values for Zn and Cd exceeded 31 and 20% of the samples, respectively. Because of the extent of the soil pollution, and the fact that this pollution spread into the surroundings by wind and through groundwater transport, this site was remediated in 2004. Obviously, this study was done before remediation. Particular attention is being paid below to the factors and processes that influence element mobility, such as soil pH, presence of spodic horizons in the subsoil, and iron oxi/hydroxides.

pH

The original soil pH in this sandy region likely varied around 4 (Scokart et al. 1983). This corresponds to the values found in the original soil profiles (pH 4–5) and in the pH_{stat} experiment (pH 3.6 after 96 h). However, pH values of up to 7.9 were measured in the polluted top soil of the Maatheide. These high pH values were found to coincide with the presence of waste materials, especially the slag material that was deposited on the site. This material strongly resembles MSWI bottom ash in composition and appearance, and it is, therefore, likely that the properties are comparable. MSWI bottom ash is typically alkaline in nature, with pH values of 11–12 due to the presence of portlandite [$Ca(OH)_2$] (Sabbas et al. 2003; Van Gerven et al. 2005). The rapidly cooled high-temperature solids that make up the MSWI bottom ash are typically metastable under natural surface conditions and will, therefore, be transformed to more stabile phases (Sabbas et al. 2003). One of the weathering reactions that occur is carbonation, the reaction of CO_2 from the air with hydroxides in the bottom ash, giving carbonates. This reaction is accompanied by a decrease in the material pH from 11–12 to 8–9 (Van Gerven et al. 2005). At pH≈8, the solubility minima are reached for most of the solid phases controlling the leaching of heavy metals such as Cd, Pb, Zn, Cu and Mo. The calcite or other carbonates that are formed can also provide a number of sorption sites for certain elements,

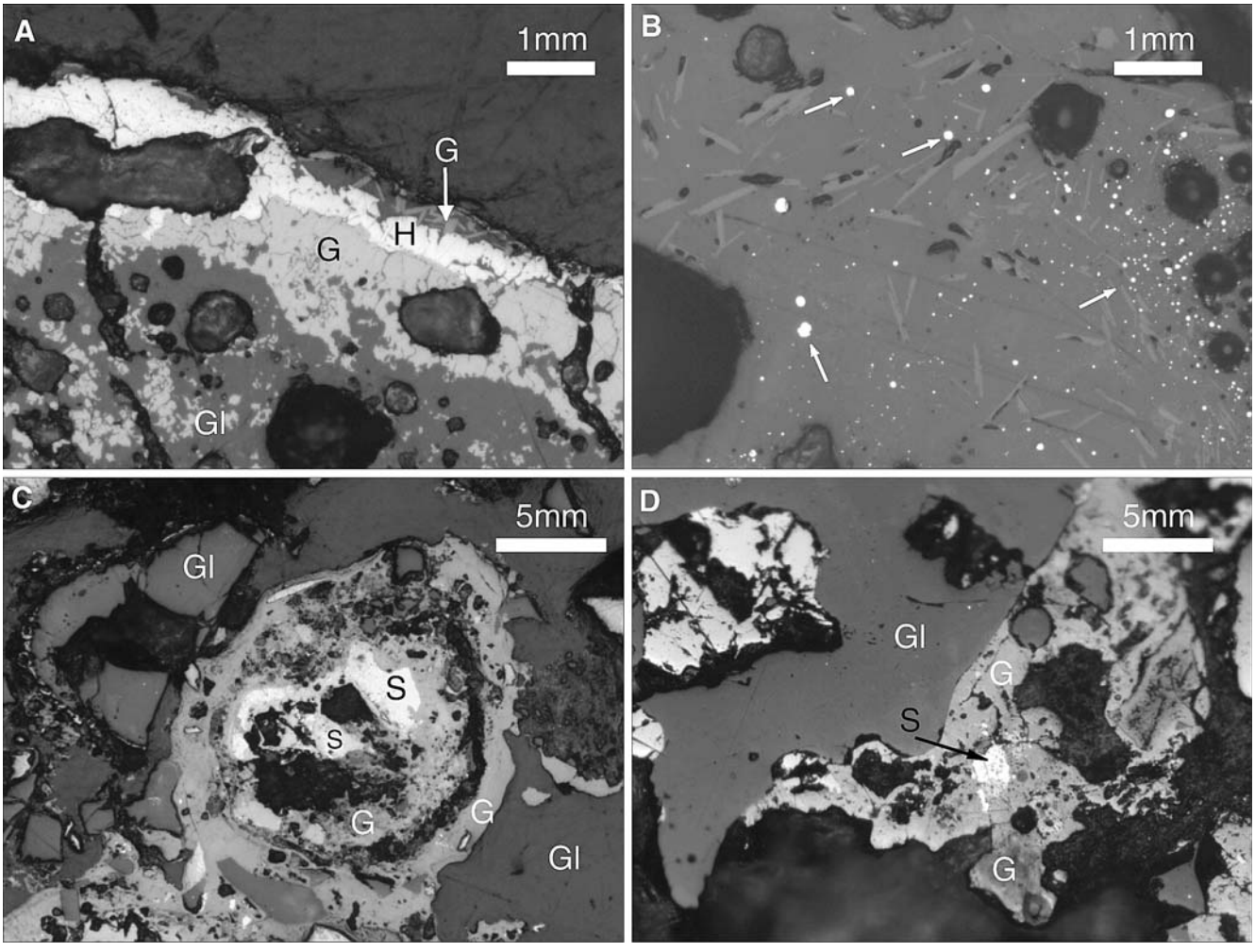

Fig. 8 **a** Outer rim of a slag fragment with clear Fe oxi/hydroxide coating (*G* goethite; *H* hematite). The inner part of the slag fragment mainly consists of glass phases (Gl); **b** glass fragment with faint exsolution phenomena, in which minute sulphide "droplets" (mainly Zn-bearing pyrite, see *arrows*) are enclosed. **c**, **d** Part of a slag fragment which partly consists of glass phases (Gl) in which sulphides (S) are enclosed. Notice that the latter are enclosed by a complex rim of Fe oxi/hydroxide [mainly goethite (G)]

e.g. Cd and Zn, that have been shown to display a high affinity for this phase (Van Gerven et al. 2004). Scavenging of heavy metals by calcite precipitation has also been observed by Ettler et al. (2005). Another possible weathering reaction is the oxidation of iron in MSWI bottom ash to iron oxi/hydroxides such as goethite (FeOOH) and hydrous ferric hydroxide [$Fe(OH)_3$]. The resulting finely crystalline phases are able to absorb and co-precipitate heavy metals including Pb, Cd, Zn, and Cu. Similar absorptive properties are also displayed by other mineral phases including aluminium (hydr)oxides and amorphous aluminosilicates (Sabbas et al. 2003). Given the similarity in composition and the presence of carbonates and other weathering products, it can be assumed that the chemical behavior of the slag materials found on the Maatheide is similar to that of aged MSWI bottom ash, and that the weathering of this slag material causes the high pH values found on the site. Alternatively, these high pH values could also be the result of the weathering of the glass phases in the slag material, which is associated with an increase of the solution pH to neutral or slightly basic values due to the exchange of elements such as Ca, Mg, Mn, Pb and Ba with the protons of the solution (Mahé-Le Carlier et al. 2000). Perret et al. (2003) also observed pH buffering conditions during the corrosion of waste glasses (pH 7–10). Whatever the buffering mechanism, the high pH values are of importance since they exert an effect on the mobility of the heavy metals under natural weathering conditions.

Spodic horizons

However, even though the heavy metals are partly adsorbed onto and retained in the mineral phases such as

carbonates, oxi/hydroxides and other secondary phases, leaching of contaminants to the subsoil occurs, as can be deduced from the pollution found in the groundwater below the site (1.4–3.2 m) (Steenackers 1991). The spodic horizon that exists in certain locations seems to be important in retaining these contaminants. The results from the soil profile distribution patterns show that heavy metals such as Cd and Zn are accumulated in the organic-rich spodic horizon. Whether this spodic horizon can really provide a means of natural attenuation for heavy metal pollution remains dubious. First of all, the development of the spodic horizon is very heterogeneous on the site, and where this layer is absent or poorly developed no accumulation is observed. Secondly, the mobility tests performed on these layers show that the heavy metals are easily remobilized. The retention is also strongly pH dependent, and a change in pH is easily induced due to the low buffering capacity of the soils (ANC for the spodic horizon is 27.5 meq/kg for a pH decrease from 3.6 to 3). Therefore, it is doubtful that this kind of natural attenuation can have a strong long-term effect on such a polluted site, especially since no adsorption is possible beyond the saturation point. In more diffusely polluted areas, it could, however, prove to be relevant in partly retaining heavy metals, or at least slow down the release of heavy metals into the environment.

Fe oxi/hydroxides

An additional factor that is of importance in retaining contaminants, are the iron oxi/hydroxides that are present on the site. As explained above, weathering of the slag materials can result in the retention of heavy metals by iron and other oxi/hydroxides. The sequential extractions that were performed, in combination with the XRD and microprobe data, confirm that significant amounts of heavy metals are bound to oxi/hydroxides.

On some of the former roads on the site, the accelerated weathering of crushed ash material has led to the development of iron crusts, similar to iron pans above ore deposits, that contain high amounts of heavy metals. Concentrations are higher than recorded in the polluted topsoil, therefore, it can be assumed that the slag materials are of a different origin. Mineralogical analysis showed that they consist mainly of Fe-oxi/hydroxides but also contain a number of sulphides like sphalerite, bornite, digenite, etc., as well as fragments of glassy slag material (Fig. 8b). The weatherability of these primary sulphides is very high under oxidizing conditions, and evidence of weathering reactions was observed, such as the transformation of pyrite to Fe-oxi/hydroxides (goethite and hematite) (Fig. 8c, d), galena to anglesite and cerussite, sphalerite to goslarite ($ZnSO_4{\cdot}7H_2O$) and/or hydrozincite ($Zn_5(CO_3)_2(OH)_6$. However, all these sulphides are presently glued together by an alteration rim of goethite, which induces a second shielding effect (Fig. 8a). This shielding is an important factor to be taken into account when modelling the heavy metal release. Even though the weathering processes are thermodynamically and kinetically possible, the shielding hampers contact with water, and the release of heavy metals is impeded.

The trapping of heavy metals in these iron oxi/hydroxides and glass phases could explain why the heavy metals are less mobile in the iron crusts than elsewhere, which was observed in the sequential extraction. The presence of Zn in the iron oxi/hydroxides was indeed confirmed by microprobe analysis. However, this seems to contradict the fact that a surprisingly small amount of heavy metals was found in the reducible (supposedly oxide-bound) fraction. A possible explanation for this is the procedure that was used for the sequential extraction, since the first step would mainly attack manganese oxides (Ure 1996), while the ammonium oxalate releases elements from amorphous iron oxides (Chao and Zhou 1983; Tipping et al. 1985; Ure 1996). Depending on the degree of crystallinity of the iron oxides, part of the heavy metals will, therefore, not be released during these extraction steps. Additionally, the amount of extractant could be insufficient to completely dissolve the components.

Finally, another potential mitigating effect of these iron crusts is that they impede drainage, and hence the leaching of heavy metals to the subsurface. Soil profiles located below and next to these iron crusts have been studied, and the concentrations of heavy metals were higher in the upper layers of the soils beneath the iron crust than those near to it. The decrease in heavy metal concentrations from the top downwards was much more abrupt for the soils under the iron crusts. This seems to indicate that leaching and removal of heavy metals is impeded and metals are retained more at the surface. Erosion by wind or water will also be reduced by the formation of an iron crust.

Conclusions

On the Maatheide (N. Belgium), the soil pollution with heavy metals was very severe, with concentrations up to percentage level for elements like Zn and Pb. Therefore, remediation was necessary (which was carried out in 2004). This study focussed mainly on the attenuation processes that took place on the site prior to the remediation, and three important factors were identified. Firstly, a pH buffering effect was noted. During their weathering process, the waste materials present on the site release heavy metals to the environment, but afterwards the pH is still high (pH 7–8) compared to the natural pH of the soils which varies around pH 4. This

pH buffering is possibly due to the carbonation of the slag material, or the weathering of the glass phases within the slags. The high pH values could influence the release time of the metals, and hence the risk to the environment. Secondly, heavy metals were found to accumulate in the strongly developed spodic horizons. However, absolute concentrations are far lower than the concentrations found in the polluted topsoil, and based on mobility tests the retention does not seem permanent. A slight pH decrease in the spodic horizons can trigger a significant release of heavy metals. This process, therefore, seems less important on severely polluted sites where remediation cannot be avoided, and where the saturation point of the spodic horizon is easily reached, but it could prove to be important in areas that are more diffusely polluted since it slows down the release of heavy metals into the environment. Finally, the shielding of the mineral phases, by encapsulation into glassy phases or Fe oxi/hydroxides is an important factor that should be taken into account in the modelling of heavy metal release and risk assessment. Due to the encapsulation, further weathering of the phases is (partially) hampered, and the release of heavy metals inhibited, even though these processes are thermodynamically and kinetically possible. Additionally, the formation of iron crusts impedes drainage, as well as erosion by wind or water. These factors should be taken into account when performing a risk assessment, since they can significantly influence the threat of heavy metal pollution to the environment.

Acknowledgments The authors would like to thank Dr. J. Vangronsveld of the 'Limburgs Universitair Centrum', W. Mennen and N. Bernaers for the information on the site and its history. Our thanks also go to Physico-Chemical Geology at the University of Leuven, in particular to Prof. W. Viaene and Prof. R Ottenburgs for the use of the XRD, D. Coetermans and H. Swevers for the chemical analysis, H. Nijs for the preparation of polished surfaces and D. Steeno for technical support. We are also grateful to G. Kayens for help with the fieldwork and mineralogical analyses, and to K. Geeraedts and A. Truyen for their practical help and the valuable discussions we had with them. This study was supported by the VIS 96–10 project. The scanning electron microscopic study was supported by a grant of 'National Fund of Scientific Research of Belgium' (project no. 2.0038.91). The corresponding author is currently working as a Research Assistant of the FWO-Vlaanderen (Fund for Scientific Research, Flanders).

References

Adriaensen W, Bouckaert J, Van Herreweghe S, Bouchat A, Swennen R (2000) Soil geochemistry in and around the town of Marche-en-Famenne (Wallonia, S-Belgium). Geologica Belgica 3(3–4):309–330

Agbenin JO, Olojo LA (2004) Competitive adsorption of copper and zinc by a B_t horizon of a savanna Alfisol as affected by pH and selective removal of hydrous oxides and organic matter. Geoderma 119:85–95

Allison JD, Brown DS, Novogradac KJ (1991) MINTEQA2/PRODEFA2, A chemical assessment model for environmental systems: Version 3.0 User's manual. Environmental research laboratory office of research and development, US-EPA, Athens

Anonymous (1990) Historiek Lommelse zinkfabriek 1904–1974. Drukkerij Lenders pvba, Lommel

Anonymous (1996) Vlaams reglement betreffende de bodemsanering—VLAREBO. Openbare Afvalstoffemaatschappij voor het Vlaams Gewest, Publicatienummer D/1996/5024/5

Bosmans H, Paenhuys J (1980) The distribution of heavy metals in the soils of the Kempen. Pedologie 30(2):191–223

Chao TT, Zhou L (1983) Extraction techniques for selective dissolution of amorphous iron oxides from soils and sediments. Soil Sci Soc Am J 47:225–232

Ettler V, Zelena O, Mihaljevic M, Sebek O, Strnad L, Coufal P, Bezdicka P (2005) Removal of trace elements from landfill leachate by calcite precipitation. In: Volume of abstracts. Seventh international symposium on the geochemistry of the Earth's surface, GES-7, August 23–27, 2005, Aix-en-Provence, France, pp 41–44

Houba VJ, Lexmond TM, Novozamsky I, Van der Lee JJ (1996) State of the art and future developments in soil analysis for bioavailability assessment. Sci Total Environ 178:21–28

Librecht IVJ, Wellens J (2002) Aardewerk-gBis. Handleiding bij het Geografisch Bodeminformatie-systeem. SADL/K.U. Leuven Research & Development, unpublished

Lombi E, Zhao F, Zhang G, Sun B, Fitz W, Zhang H, McGrath SP (2002a) In situ fixation of metals in soils using bauxite residue: chemical assessment. Environ Pollut 118:435–443

Lombi E, Zhao F, Wieshammer G, Zhang G, McGrath SP (2002b) In situ fixation of metals in soils using bauxite residue: biological effects. Environ Pollut 118:445–452

Lombi E, Hamon RE, McGrath SP, McLaughlin MJ (2003) Lability of Cd, Cu and Zn in polluted soils treated with lime, beringite and red mud, and identification of non-labile colloidal fraction of metals using isotopic techniques. Environ Sci Technol 37(5):979–984

Mahé-Le Carlier C, Le Carlier de Veslud C, Ploquin A, Royer J (2000) Natural weathering of archaeo-metallurgical slags: an analog for present day vitrified wastes. Earth Planet Sci 330:179–184

McLean JE, Bledsoe BE (1992) Behaviour of metals in soils, Office of solid waste and emergency response (US EPA) EPA/540/S-92/018

Mench MJ, Didier VL, Löffler M, Gomez A, Masson P (1994). A mimicked in situ remediation study of metal-polluted soils with emphasis on cadmium and lead. J Environ Qual 23:58–63

Nelson DW, Sommers LE (1982) Chapter 29: total Carbon, organic carbon, and organic matter. In: Page AL, Miller RH (eds) Methods of soil analysis. Part 2-chemical and microbiological properties. Number 9 (Part 2) in the series Agronomy. American Society of Agronomy, Inc., Madison, pp 539–579

Perret D, Crovisier JL, Stille P, Shiels G, Mäder U, Advocat T, Schenk K, Chardonnens M (2003) Thermodynamic stability of waste glasses compared to leaching behaviour. Appl Geochem 18:1165–1184

Quevauviller P, Rauret G, Ure A, Bacon J, Muntau H (1997) The certification of the EDTA- and acetic acid-extractable contents (mass fractions) of Cd, Cr, Cu, Ni, Pb and Zn in sewage sludge amended soils. ECSC-EC-EAEC. EUR 17127 EN, Brussels

Sabbas T, Polettini A, Pomi R, Astrup T, Hjelmar O, Mostbauer P, Cappai G, Magel G, Salhofer S, Speiser C, Heuss-Assbichler S, Klein R, Lechner P (2003) Management of municipal solid waste incineration residues. Waste Manage 23:61–88

Scokart PO, Meeus-Verdinne K, De Borger R (1983) Mobility of heavy metals in polluted soils near zinc smelters. Water Air Soil Pollut 20:451–463

Spark KM, Johnson BB, Wells JD (1995) Characterizing heavy metal adsorption on oxides and oxyhydroxides. Eur J Soil Sci 46:621–631

Steenackers J (1991) Verkennend onderzoek van de kwaliteit van bodem en grondwater op de Maatheide te Lommel, Tussentijds verslag. IREA (Instituut voor Reddingswezen, Ergonomie en Arbeidshygiëne)

Swennen R, Van der Sluys J, Hindel R, Brusselmans A (1998) Geochemistry of overbank and high-order stream sediments in Belgium and Luxemboug: a way to assess environmental pollution. J Geochem Explor 62:67–79

Tack FM, Verloo MG (1995) Chemical speciation and fractionation in soil and sediment heavy metal analysis: a review. Int J Environ An Ch 59:225–238

Tessier A, Campbell PG, Bisson M (1979) Sequential extraction procedure for the speciation of particulate trace metals. Anal Chem 51(7):844–851

Tipping E, Hetherington NB, Hilton J, Thompson DW, Bowles E, Hamilton-Taylor J (1985) Artifacts in the use of selective chemical extraction to determine distributions of metals between oxides of manganese and iron. Anal Chem 57:1944–1946

Ure AM (1996) Single extraction schemes for soil analysis and related applications. Sci Total Environ 178:3–10

Van Gerven T, Van Baelen D, Dutré V, Vandecasteele C (2004) Influence of carbonation and carbonation methods on leaching of metals from mortars. Cement Concrete Res 34:149–156

Van Gerven T, Van Keer E, Arickx S, Jaspers M, Wauters G, Vandecasteele C (2005) Carbonation of MSWI-bottom ash to decrease heavy metal leaching, in view of recycling. Waste Manage 25:291–300

Vangronsveld J, Sterckx J, Van Assche F, Clijsters H (1995a) Rehabilitation studies on an old non-ferrous waste dumping ground: effects of revegetation and metal immobilization by beringite. J Geochem Explor 52:221–229

Vangronsveld J, Van Assche F, Clijsters H (1995b) Reclamation of a bare industrial area polluted by non-ferrous metals: in situ metal immobilization and revegetation. Environ Pollut 87:51–59

Vangronsveld J, Colpaert JV, Van Tichelen KK (1996) Reclamation of a bare industrial area polluted by nonferrous metals: Physico-chemical and biological evaluation of the durability of soil treatment and revegetation. Environ Pollut 94:131–140

Xiao-Quan S, Bin C (1993) Evaluation of sequential extraction for speciation of trace metals in model soil containing natural minerals and humic acid. Anal Chem 65:802–807

Zevenbergen C, Van Reeuwijk LP, Bradley JP, Bloemen P, Comans RN (1996) Mechanisms and conditions of clay formation during natural weathering of MSWI bottom ash. Clay Clay Miner 44(4):546–552